Local and long-range order of carbon impurities on Fe(100): Analysis of self-organization at a nanometer scale

G. Panaccione, J. Fujii, and I. Vobornik
TASC Laboratory INFM-CNR, in Area Science Park, S.S.14, Km 163.5, I-34012 Trieste, Italy

G. Trimarchi and N. Binggeli
INFM-CNR DEMOCRITOS National Simulation Center and Abdus Salam International Center for Theoretical Physics, I-34014 Trieste, Italy

A. Goldoni and R. Larciprete
Sincrotrone Trieste S.C.p.A., Lab. ELETTRA, in Area Science Park, S.S. 14 Km 163.5, I-34012 Trieste, Italy

G. Rossi
TASC Laboratory INFM-CNR, in Area Science Park, S.S.14, Km 163.5, I-34012 Trieste, Italy
and Dipartimento di Fisica dell' Universita' di Modena e Reggio Emilia, I-41100 Modena, Italy
(Received 8 August 2005; revised manuscript received 20 October 2005; published 26 January 2006)

Bulk carbon impurities segregate at the Fe(100) surface and, upon thermal annealing, can form metastable surface phases, with local and long-range order, that show peculiar electronic properties. We present a surface science study of C-segregated Fe(100) with scanning tunneling microscopy/spectroscopy (STM/STS), core level spectroscopy, and *ab initio* calculations of the surface structure. In particular, we investigate a $c(3\sqrt{2}\times\sqrt{2})$ structure, observed for 0.67 ± 0.05 atomic layers of C segregated at the iron surface. This structure is found to be due to self-organized carbon stripes, which form a regular pattern on a nanometer lateral scale and are made of zig-zag chains. The C atoms in the chains lie slightly off center in the fourfold hollow site and are bonded to 5 Fe neighbors. Striking features of this structure are the self-avoiding chains, the passivation effect of the iron surface, and the presence of one-dimensional-like Fe surface states close to the Fermi energy.

DOI: 10.1103/PhysRevB.73.035431 PACS number(s): 68.65.−k, 73.20.−r, 73.22.−f

I. INTRODUCTION

Self-organized nanostructures grown onto solid samples are nowadays not only one of the most promising fields of application for new technologies but also crucial systems for the understanding of the physical properties at a nanoscale level,[1] in particular in materials where strong implications on the electronic and magnetic properties are expected and observed. Recent results on single-crystal stepped surfaces clearly demonstrated, both experimentally and theoretically, that a large number of self-organized structures can be "constructed" with regular shape and distances by an appropriate control of the growth processes.[1–4]

Surface segregation of bulk impurities is driven by the total energy minimization of the solid that reduces its total structural stress by transferring it into the surface layer, up to surface concentrations that can be accommodated into low-energy metastable structures.[5,6] The surface reconstructions induced by segregation are therefore a special case of global self-assembly of the real solid. Segregation of bulk impurities starts as a diffusive phenomenon and as such can be activated by increasing the solid temperature, a procedure conventionally called annealing that represents a fundamental step in the preparation of atomically clean, flat, and ordered surfaces of a single crystal. Often the preparation of an "ideal" surface of a transition metal is accompanied by a detectable amount of segregation of bulk impurities which therefore contributes to the actual properties of the "clean surface." Saturation concentrations of segregated species determine some metastable surface phases that prevent further segregation, or segregation of other species, at a given temperature, even for prolonged annealing. These structures are therefore of thermodynamic interest for the whole solid and are often characterized by well-defined local and long-range order, i.e., by surface reconstruction.[7–9] This is the case, in particular, of the Fe(100) surface enriched with C segregated from the bulk. The clean bcc Fe(100) surface does not show substantial surface relaxation and/or reconstruction,[10] but segregation of impurities such as Si, C, P, S, and N, generally incorporated into the surface fourfold hollow sites, leads to a $c(2\times2)$ reconstruction for impurity abundance of about half a monolayer.[8,11]

Here we address the atomic and electronic structure of the C/Fe(100) segregated system, with particular attention to a metastable phase of higher C concentration than the $c(2\times2)$. This peculiar phase is characterized by the formation of stripes involving zig-zag chains of C atoms and the Fe confined within. We present the results obtained with core level spectroscopies for abundance determination and with scanning tunneling microscopy/spectroscopy (STM/STS) for local order determination; moreover, *ab initio* calculations are presented to refine the atomic structure, to better understand the origin of the formation of the C chains, and to assign the tunneling current maxima to specific electron states of the surface. Our results suggest that the formation of the zigzag pattern, observed at a C coverage of $\frac{2}{3}$ monolayer, derives

from repulsive interactions between C impurities segregated at hollow sites of the Fe(100) surface.

II. EXPERIMENTAL AND THEORETICAL METHODS

Fe(100) surfaces of bcc Fe\3%Si single crystals with miscut lower than 1 deg were cleaned by sputtering (800 V, Ar^+) and annealing cycles, and subsequently enriched in segregated species by calibrated annealings. The surfaces presented flat [100] terraces typically 100 Å wide, separated by monoatomic steps. Segregation of silicon, carbon, and phosphorus were promoted by annealing. Silicon enrichment at the surface was only observed at the early stages of the crystal preparation. A reproducible regime of segregation, for subsequent treatments, was established: carbon-rich surfaces were obtained for annealing temperatures in the 650 K to 850 K range, and phosphorus enrichment was obtained from 800 K to 950 K. The observed reconstructed surface structures due to C, without detectable traces of P, could be reproduced routinely. More details about the preparation of the samples can be found in Ref. 12.

The experiments were performed mainly on the APE-INFM surface laboratory and beamlines at the ELETTRA storage ring of Sincrotrone Trieste.[13] Sample preparation and analysis by low-energy electron diffraction (LEED), Auger electron spectroscopy, and scanning tunneling microscopy (STM) were performed in a base vacuum of 4×10^{-11} mbar. The STM tip was electrochemically etched (1 N NaOH solution) from tungsten wire and finally cleaned by sputtering-annealing cycles *in situ*. All the STM images presented here were obtained in constant current mode. The core level data were obtained, on replica samples, at the SuperEsca beamline equipped with a double-pass hemispherical analyzer, operated at an overall energy resolution of 200 meV and angular resolution of ±2 degrees.

The *ab initio* calculations were performed within the general gradient approximation (GGA) to density functional theory, using the pseudopotential plane-wave method. We employed the spin-polarized GGA exchange-correlation functional of Perdew, Burke, and Ernzherof[14] and Vanderbilt ultrasoft pseudopotentials.[15–18] The surfaces were modeled using a slab geometry in supercells containing nine layers of Fe and nine equivalent layers of vacuum. The Fe slab was generated using the theoretical value of the equilibrium lattice parameter of bcc Fe: $a=2.86$ Å (the experimental value is 2.87 Å). We placed the C impurities on both sides of the Fe slab, in order to preserve the equivalence by reflection σ_h of the two surfaces in the supercell. Plane waves with a kinetic energy up to 27 Ry were included in the basis set for the expansion of the electronic orbitals, and with a kinetic energy up to 270 Ry for the expansion of the electronic charge density (including the core-augmentation charge).[15] The integrations in reciprocal space were performed using a (2,6,1) Monkhorst-Pack[19] *k*-point grid. A Gaussian electronic-level smearing with full width at half maximum of 0.02 Ry was used to determine the Fermi energy. The atomic structure of the C/Fe(100) surfaces was relaxed, keeping the three innermost layers of the slab frozen at their bulk positions. The relaxation process was stopped when the forces on the atoms were smaller than 0.001 Ry/a.u.

To complement the *ab initio* calculations, and help in understanding the mechanism responsible for the formation of the C chains, we also carried out classical Monte Carlo simulations, based on a model Hamiltonian. The model Hamiltonian was written in terms of pairwise interactions between carbon impurities sitting at hollow sites of the Fe (001) surface:

$$H = U_{1N}\sum_{\langle i,j\rangle:1N} n_i n_j + U_{2N}\sum_{\langle i,k\rangle:2N} n_i n_k + U_{3N}\sum_{\langle i,l\rangle:3N} n_i n_l, \quad (1)$$

where $n_i=1,0$ is the occupation variable of site i. The sum in the first, second, and third terms on the right-hand side of Eq. (1) runs over first, second, and third nearest-neighbor hollow sites of the Fe surface, respectively, and U_{jN} stands for the jth nearest-neighbor C-C interaction (considered up to the third nearest neighbor). For a given set of interaction parameters, U_{jN}, we determined the lowest-energy configuration(s) of Eq. (1), for a given C coverage, by Monte Carlo simulated annealings using periodic boundary conditions (with unit cells including up to 30×30 hollow sites).[20]

III. RESULTS

A. XPS, Auger, LEED, STM

Carbon 1*s* core level spectra for Fe(100) samples with different degrees of C segregation are presented in Fig. 1. The right panel shows comparison of the C 1*s* line shapes. The residual C on the as-sputtered iron surface shows a main C 1*s* line at 283 eV of binding energy (BE) and further lines at ~1.6–1.8 eV higher BE, i.e, at binding energies comparable to those of graphite (284.4 eV) and of bulk diamond (285.0 eV).[21] The lower binding energy of the main peak with respect to graphite is due to the strong polarity of the carbon-iron bonds.[8] In the left panel we present an on-line sequence of C 1*s* spectra acquired as the annealing temperature increases from room temperature to 900 K, along the three relevant axes. The main C 1*s* line shifts to lower BE by ≃0.7 eV as the annealing proceeds. The intensity changes are connected with the kinetics of the segregation process: as the temperature is raised above RT, the initial graphitic component vanishes while the main component at lower BE shifts in energy and loses the shoulder structure.[22] The C 1*s* intensity reaches the maximum at 600 °C and decreases for higher temperatures due to the onset of the segregation of other impurities that substitute C in the hollow site. The maximum intensity of C 1*s* corresponds to the formation of the zig-zag chain surface structure.

Typical Auger spectra and LEED patterns for relevant segregation temperatures, as obtained in Ref. 12, are presented in Fig. 2. Carbon, silicon, and sulfur form $c(2\times2)$ superstructures on Fe(100) upon surface segregation and occupancy of the fourfold hollow sites.[8,23] A clear $c(2\times2)$ LEED pattern is observed in panel (a) after annealing at 300 °C for 8 min, due to the segregation of C. For such surfaces the $(\frac{1}{2},\frac{1}{2})$ LEED spots are faint and quite broad. By increasing the annealing time one observes a sharpening and an increased brightness of the LEED spots, to which corresponds a higher ratio in the Auger C KLL vs. Fe LMM line

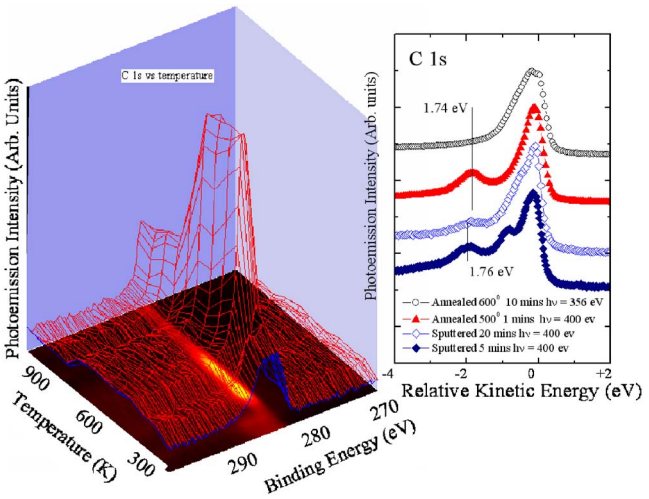

FIG. 1. (Color online) Left panel: Polar plot of the C 1*s* photoemission intensities versus temperature, as measured at $h\nu$ =400 eV. Spectra are normalized to the maximum intensity. In the bottom panel, the projection of the C 1*s* intensity is shown. The evolution of the segregation reveals a first phase in which the graphitic-like carbon shifts towards the main line; subsequently, the intensity of the main line reaches a maximum, correspondng to the formation of the zig-zag chains, followed by a decrease of intensity due to the appearance of the next segregated impurity (in the present case, phosphor). Right panel: Carbon 1*s* Core level photoemission ($h\nu$=400 eV) as a function of annealing temperature. Spectra are normalized to the intensity of the main line. The leading edge is found at $E_{binding} \approx 283$ eV, well in agreement with the predicted 2 eV shift with respect to the graphite binding energy (BE =284.7) (from Ref. 8). Two components are visible in the spectra: the one at higher binding energy clearly disperses towards the main line during annealing.

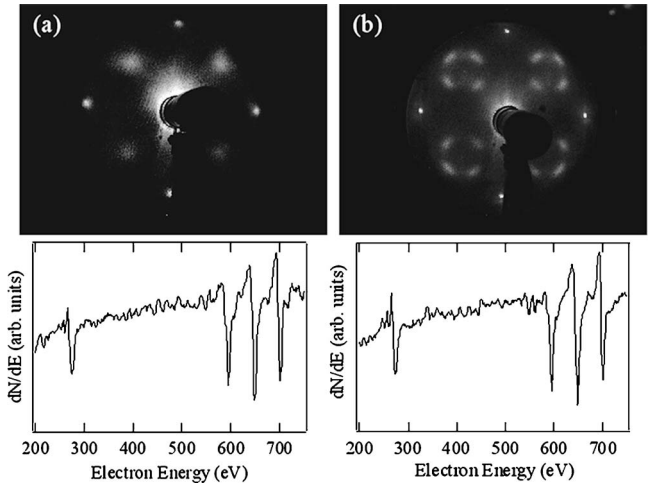

FIG. 2. LEED patterns and AES spectra of the C/Fe(100) surfaces after annealing (a) 8 min at 300 °C, (b) 4 min at 550 °C. Electron energy is 48 eV for both LEED images. In (a), a clear $c(2\times2)$ reconstruction is visible, and the ratio between C KLL and Fe LMM auger lines correspond to 0.5 ML coverage of carbon. In (b), the $(\frac{1}{2},\frac{1}{2})$ spots of $c(2\times2)$ are split and the LEED shows a $c(3\sqrt{2}x\sqrt{2})$ reconstruction. C coverage is 0.67 ML from the corresponding Auger spectrum. In the Auger spectrum corresponding to LEED of panel (b), one notices the up-down feature of the main line and the two structure at lower kinetic energy, not present in the Auger spectrum of case (a).

intensities. By raising the annealing temperature up to 550 °C, the $c(2\times2)$ pattern is gradually substituted by a new $c(3\sqrt{2}\times\sqrt{2})$ pattern [Fig. 2(b)]. In the new LEED pattern four elongated spots replace the broad $(\frac{1}{2},\frac{1}{2})$ spots of $c(2\times2)$. The Auger line shape of carbon corresponding to (b) presents two structured peaks at lower kinetic energy than the main line, when compared to the Auger line relative to the $c(2\times2)$ LEED. Assuming 0.50±0.05 ML C coverage relative to the $c(2\times2)$ LEED patterns [Fig. 2(a)], the coverage for the $c(3\sqrt{2}\times\sqrt{2})$ reconstruction is estimated to be 0.67±0.05 ML. The $c(3\sqrt{2}\times\sqrt{2})$ reconstruction was reported for C/Mo(100) and C/W(100) surfaces, with split spots of higher brightness with respect to the present ones.[24,25] The superstructure visible in Fig. 2(b) displays a stretched circle along the ⟨100⟩ direction and a spot lenght of $\simeq\frac{1}{7}$ of the (1×1) square: this indicates the presence of domains with approximately 2 nm lateral dimensions.

We present in Fig. 3(a) the STM image (V_b=+400 mV, I_t=0.1 nA) of a surface area of 165×165 Å^2: stripes appear with regular spacing on a flat terrace 100 Å wide. The stripes are oriented along the ⟨11⟩ or ⟨1-1⟩ directions. Their length does not exceed 2 nm between terminations or 90 deg rotations, consistent with the elongation of the LEED spots. A 26×26 Å^2 STM image in Fig. 3(b) shows the breaking point of the stripes. A shift is clearly seen, placed approximately at $\frac{1}{3}$ of the distance between two stripes. This phase shift is responsible for the anisotropic stretching of the LEED superlattice spots in one preferential direction. The line breaking gives rise to a white cloud in the STM image, in Fig. 3(a), which develops along the breaking points of the stripes [see Fig. 3(b)].

More can be learned about the atomic details of the $c(3\sqrt{2}\times\sqrt{2})$ structure by inspection of Fig. 4. Panels (a) and (b) show the same area of 33×33 Å^2 as measured by STM with two different bias voltages (negative and positive bi-

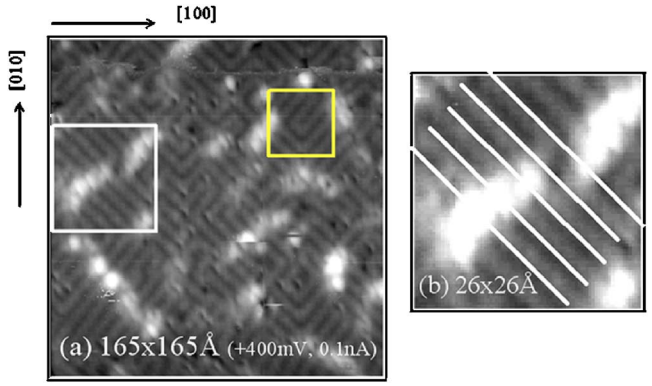

FIG. 3. (Color online) (a) 165×165 Å^2 STM image of C/Fe(100) as from the LEED image in Fig. 1(b), obtained with a 4 min annealing at 550 °C. V_b=+400 mV, I_t=0.1 nA. The line structure is along the ⟨11⟩ direction and the length reaches a maximum of 20 Å before a 90 deg rotation or a break point. (b) Zoom of 26×26 Å^2 of the marked area in bottom left part of Fig 2(a), showing the shift of the carbon lines. White lines are guides for the eyes.

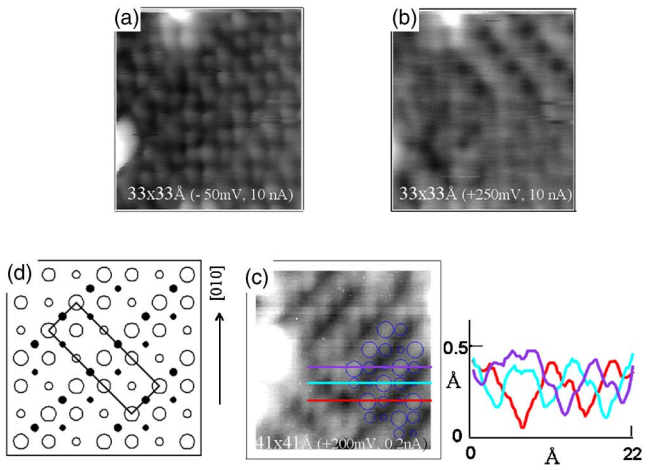

FIG. 4. (Color online) Atomically resolved STM images with different bias voltage and current condition, for C/Fe(100) surfaces obtained as in Fig. 3. (a), (b) Same 33×33 Å^2 area and $I_t=10$ nA, but respectively $V_b=-50$ mV and $V_b=+250$ mV. The line arrangement of Fig. 3 is better revealed by the condition of panel (b). The distances are compatible with the bcc Fe atoms in the (100) plane (2.87 Å). (c) Atomically resolved 41×41 Å^2 STM image ($V_b=+200$ mV, $I_t=0.2$ nA) showing the zig-zag arrangement of the lines, corresponding to the box indicated in the top right part of Fig. 3. The distance between nearest neighbor atoms is 2.9 Å. The cross sections along the three lines of the images show the presence of a difference in height of about 0.1 Å in the atoms. Circles reproduce the arrangement of panel (d). (d) Schematic spheres drawing of the carbon $c(3\sqrt{2}x\sqrt{2})$ reconstruction. The unit cell corresponds to the black rectangle. Large and small white (black) circles correspond to lower and higher iron (carbon) atoms.

ases, respectively). In panel (a) one observes a regular (1×1) distribution of bright spots, whose relative distance compares well with the spacing of bcc Fe atoms in the (100) plane (2.87 Å). On the other hand, in panel (b) one observes a stripe arrangement similar to Fig. 3. Comparison between the locations of the maxima of the STM signal, in Figs. 4(a) and 4(b), suggests that the stripe signal in the STM images at positive bias is mostly related to Fe atoms. It is important to note that the values of the bias voltage used in the STM images of Figs. 3, 4(b), and 4(c) are comparable to or larger than the value of the Fe surface state peak of the clean Fe(001) surface, as measured by STS (at ~0.2 eV above the Fermi energy).[26,27] A confinement[27] and a shift to higher energy[27,28] of such surface states have been previously observed in surfaces with segregated elements.

The atomically resolved topography image in panel (c) (size 41×41 Å^2, $V_b=+200$ mV, $I_t=0.2$ nA, corresponding to the top right box in Fig. 3) reveals that the stripes of Fig. 3(a) do have a zig-zag atomic fine structure. As already reported in Ref. 12, the distance between the nearest-neighbor atoms (bright spots) in the zig-zag chains is $\simeq2.90\pm0.05$ Å, to be compared with the distance of two bcc Fe atoms in the (100) plane (2.87 Å). A further analysis with respect to previous results is presented with a cross-section analysis [right of panel (c)], showing a slight difference in the height position (corrugation) within the zig-zag chains: lower and higher positions are found at 0.10 ± 0.05 Å one from the

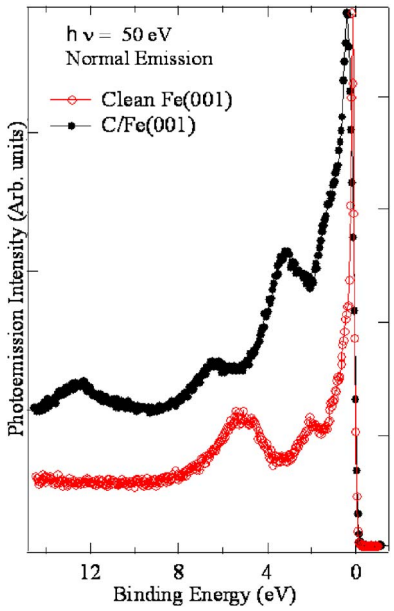

FIG. 5. (Color online) ARPES data on C/Fe(100) at $h\nu=50$ eV. (a) Comparison of the valence band spectra measured at normal emission for reference/pure Fe (red curve) and C/Fe(100) (black curve). The pure Fe(001) spectrum has been measured on a Fe crystalline thick film (3000 Å) grown on MgO substrate. The oxygen related feature at 6 eV BE for pure Fe as well as the carbon related one at 12 eV for C/Fe(100) represent the main difference between the spectra.

other. This corrugation may correspond to nonequivalent electronic density at different positions. White regions are observed at the break point of zig-zag chains, possibly corresponding to the presence of unsaturated bonds. A sketch of the proposed carbon $c(3\sqrt{2}x\sqrt{2})$/Fe(100) structure is shown in panel (d). Small and large white(black) circles represent iron(carbon) atoms. The unit cell contains four atoms, corresponding to a C coverage on Fe(100) of 0.67 ML, well in agreement with Auger data. Annealing at higher temperatures promotes also P segregation.[12] We remind that P atoms stick first to the corner of the zig-zag chains [with an estimated coverage of 0.2 equivalent ML on Fe(100)], presumably where unsaturated bonds of the underlying surface are available; in fact, the number of white "clouds" is strongly reduced after P segregation which indirectly supports the attribution. At saturation almost all the terraces are covered by the P atoms chains. The P segregated surface is characterized by long chains with nonperiodic arrangement [panel (c)] and no long-range order.[12]

Finally, in Fig. 5 we present angular resolved photoemission (ARPES) spectra, where we compare atomically clean Fe(001), as grown by MBE on MgO, and the $c(3\sqrt{2}\times\sqrt{2})$ C/Fe(100) surface. Data were obtained *in situ* at the APE-LE beamline[13] equipped with a SES2002 analyzer: the overall energy resolution was set to 20 meV and the angular resolution was ±0.2 degrees. ARPES spectra were measured at normal emission with linearly polarized light of $h\nu=50$ eV and integrated over ±4 deg about Γ (normalized to the maximum intensity). In the reference Fe(001) (red curve) the peak at ~5.5 eV BE is due to residual oxygen contamination. No

structures are present at higher binding energies. The oxygen contamination was unavoidable after surface preparation at a residual pressure of 1×10^{-10} mbar and further increased with time. By calibrating the photoemission intensities by the relative Fe $3d$ and O $2p$ photoionization cross section at $h\nu=50$ eV (Ref. 29) the amount of oxygen contamination of the Fe(001) surface was of ≈0.2 monolayers. The C/Fe(001) valence band shows a broader main band with prominent features in the 1–5 eV BE range. At ~6 eV BE there is a peak and an extra peak appears at 12 eV BE. Contrary to the reference Fe(001), the intensity of the peak at 6 eV does not change with time in UHV. In the vicinity of the Fermi energy the main contribution to the photoemission intensity comes from the Fe d bands and from an intense surface state, in the case of the pure Fe. However, we also observed important modifications of the Fe(001) Fermi surface in the presence of C chains that will be discussed elsewhere.[30]

The ensemble of the STM and spectroscopic observations on the $c(3\sqrt{2}\times\sqrt{2})$ C/Fe(100) surface indicates that the electronic structure of the iron surface is severely modified by the presence of the C atoms, and the lateral zig-zag charge density stripes with vertical corrugation and free charge at the breaking points or at the 90 deg turning points all indicate that a special bonding configuration is established involving carbon and iron surface atoms. Such configurations at segregated surfaces should not necessarily be understood as stable chemical configurations since the interface energy with the bulk probably plays an important role in determining the saturation and the energy barriers for further surface enrichment in segregated species. Previous STM experiments on transition metal surfaces have already pointed out the influence of C on the local density of states.[28,31] It is therefore appropriate to conduct the analysis of the STM by performing electron state calculations on structural models compatible with the experimental data.

B. Calculations: $c(3\sqrt{2}\times\sqrt{2})$ reconstructed structure

In Fig. 6, we display the equilibrium atomic structure obtained from the *ab initio* calculations for the C/Fe(100) $c(3\sqrt{2}\times\sqrt{2})$ surface, starting from the carbon arrangement suggested by STM and LEED results (model in Fig. 4). We note that in the starting configurations, we imposed two different heights (differing by 0.1 Å) for the two inequivalent C atoms within the chains and used several different initial values for the average distance between the C atoms and the Fe surface, ranging from +0.5 Å (i.e., above) to −0.2 Å (below) the Fe surface layer. In all cases, the same equilibrium atomic structure (Fig. 6) was found, with all C atoms sitting at equivalent positions. We also started from configurations in which the two C atoms within the chains are laterally displaced one with respect to the other, in order to break all possible σ_v reflection symmetries of the $c(3\sqrt{2}\times\sqrt{2})$ reconstructed surface; also in this case we recovered the structure shown in Fig. 7. In this relaxed structure, the C atoms are located very close to the Fe surface layer, i.e., only ~0.21 Å (0.32 Å) higher than the outermost (second outermost) Fe atoms, and exhibit a small lateral displacement with respect to the center of the Fe(100) hollow site. Each carbon atom has five nearest-neighbor Fe atoms, with C-Fe distances ranging from 1.89 to 2.05 Å. The closest Fe atom (at 1.89 Å) is located just below the C atom, i.e., within the second Fe layer from the surface. The other four nearest neighbors belong to the outermost Fe layer: two are located at 1.96 Å along the C chain and two at 2.05 Å along the direction perpendicular to the C chains. We note that the equilibrium C-C (Fe-Fe) nearest-neighbor distance within the zig-zag stripes is 3.01 Å (2.62 Å), i.e., increased by 5% (decreased by 8%) relative to the Fe bulk equilibrium value of 2.86 Å.

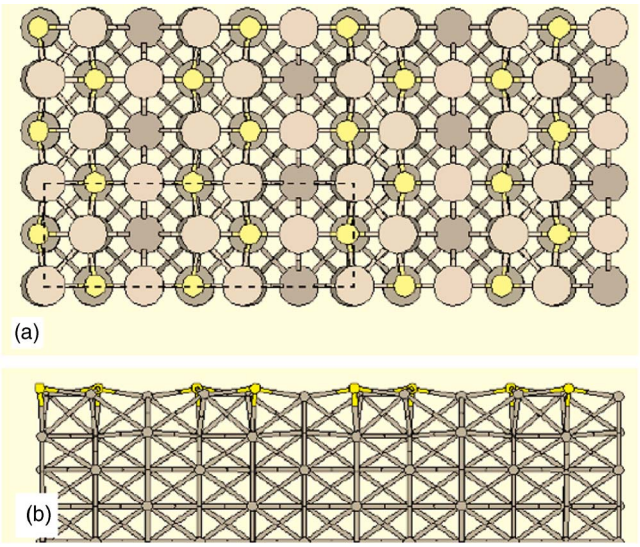

FIG. 6. (Color online) Theoretical equilibrium atomic structure of the C/Fe(100) $c(3\sqrt{2}\times\sqrt{2})$ reconstructed surface with a C coverage of $\frac{2}{3}$ monolayer. Top (a) and side (b) views. Small/large circles correspond to C/Fe atoms in (a).

We have examined the relative stability of the zig-zag chain configuration with the C atoms on hollow (H) sites (Fig. 6), with respect to similar configurations having the C atoms located either on bridge (B) sites or on top (T) sites. We rigidly displaced the C zig-zag chains, parallel to the Fe surface plane, from the H to the B or T sites, and let the corresponding atomic structure fully relax. The resulting relaxed B and T structures were found to be considerably higher in energy than the relaxed H configuration, i.e., by respectively ~2 and ~3 eV per carbon atom. Therefore, the *ab inito* results confirm that the C atoms in the zig-zag chain structure sit at hollow sites and show that they very strongly bind to the Fe(100) surface at such sites. This is consistent with the results of a recent *ab initio* study of isolated C atoms on Fe(100) (Ref. 32) and with the analysis of LEED experiments on the $c(2\times2)$ C/Fe(100) surface,[23] which also both show that the C atoms sit in the hollow position with a fivefold coordination.

In order to better understand the origin of the formation of the C zig-zag chains, we have performed total-energy calculations for selected C arrangements illustrated in Fig. 7. Such configurations include either 2 or 3 C [110] rows per $c(3\sqrt{2}\times\sqrt{2})$ surface cell. The corresponding relative energies (at fixed C coverage) are also given in Fig. 8 for the fully relaxed structures. The results for the two-row structures

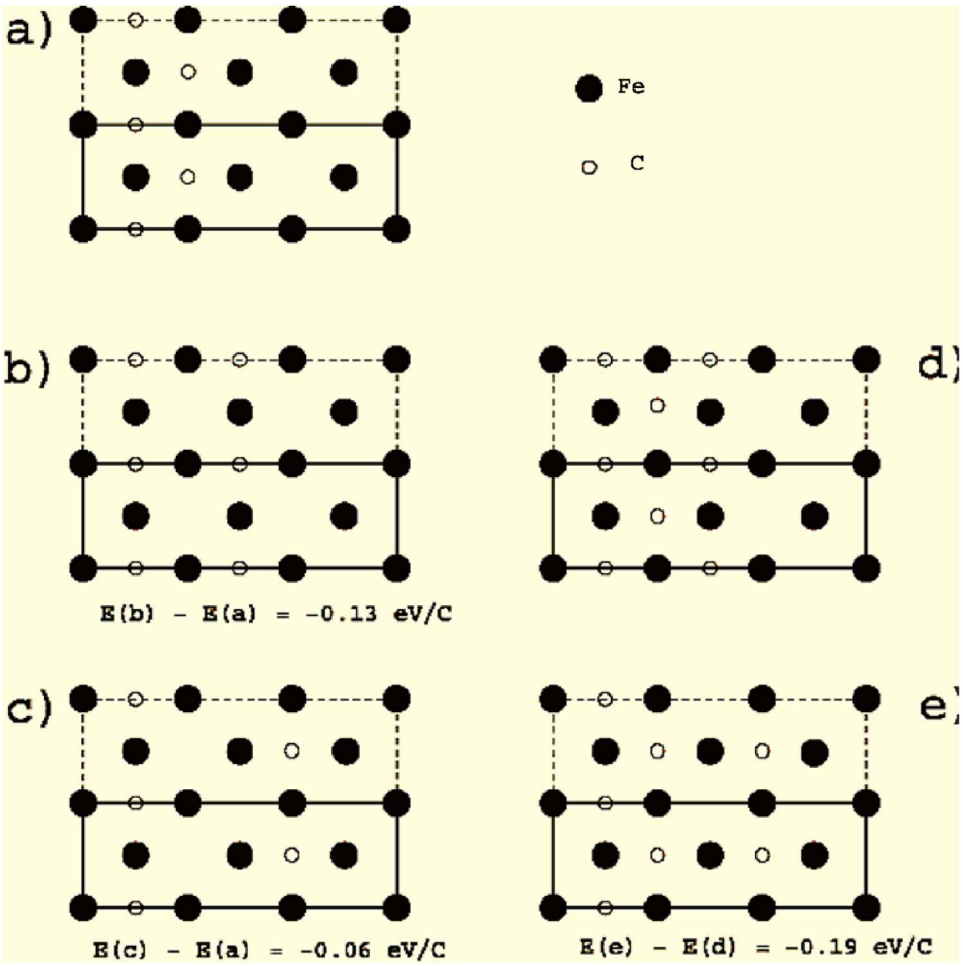

FIG. 7. (Color online) Schematic representation of the C/Fe(100) surfaces with two C rows [configurations (a), (b), and (c)], and with three C rows [configurations (d) and (e)] per $c(3\sqrt{2}\times\sqrt{2})$ surface cell considered in the *ab initio* calculations. For all the configurations, two cells are represented, and the fundamental cell is indicated by the solid line. The corresponding calculated relative energies are also given.

show that the zig-zag chain [two adjacent rows, configuration (a)] in Fig. 3 is actually less stable (by respectively ~0.13 and ~0.03 eV per C) than the configurations (b) and (c), which exhibit a larger separation between the C rows. Similarly, for the three-row structures, the configuration (d) with three adjacent rows is much less stable (by ~0.19 eV per C) than the configuration (e) in which one of the rows is further apart from the other two. These results indicate that the C zig-zag chain is by no means a stable entity, two isolated C rows are energetically more favorable than a zig-zag chain, and that the C rows exhibit repulsive nearest-neighbor interactions. We note that this supports the assumption of repulsive C-C pairwise interactions made in previous model-simulation studies of C segregation on Fe(100),[7] which account for the experimental $c(2\times2)$ structure, corresponding to a half-coverage situation. Furthermore, on the basis of similar Monte Carlo simulations, using the model Hamiltonian in Eq. (1) and performing simulated annealings, we find that the C zig-zag chain structure in Fig. 6 is actually the single lowest-energy configuration that can be obtained with the contraints that (*i*) the C coverage is $\frac{2}{3}$ monolayer, (*ii*) the C atoms occupy hollow sites, and (*iii*) the C-C interactions are repulsive up to the third-nearest neighbor (neglecting interactions beyond third-nearest neighbor). The formation of the $c(3\sqrt{2}\times\sqrt{2})$ zig-zag structure, observed at a C coverage of $\frac{2}{3}$ ML, can thus be explained in terms of a minimization, at that given coverage, of repulsive interactions between C impurities occupying hollow sites.

It is noteworthy that when repulsive interactions are included only up to first- or second-nearest neighbor, the zig-zag chain structure is only one among the many possible degenerate ground-state configurations. The interactions which stabilized the zig-zag chain structure appear thus to have some long-range character, which could have an electrostatic and/or elastic origin. Howevever, further investigations are needed to assess the exact origin of these interactions.

IV. DISCUSSION

A. C surface segregation

The core level photoemission data show that the impurity diffusion towards the surface can be kinetically driven by annealing procedures and that a sequence of metastable phases can be reached and carefully reproduced many times, i.e., the bulk represents an infinite reservoir of impurity atoms. The C concentration at the surface reaches a maximum at $\frac{2}{3}$ of a monolayer, to which corresponds a well-defined metastable phase that changes severely the electronic properties of the iron surface, for example reducing the reactivity with colliding molecules of the residual gas. In particular, the surface appears passivated with respect to oxydation. Moni-

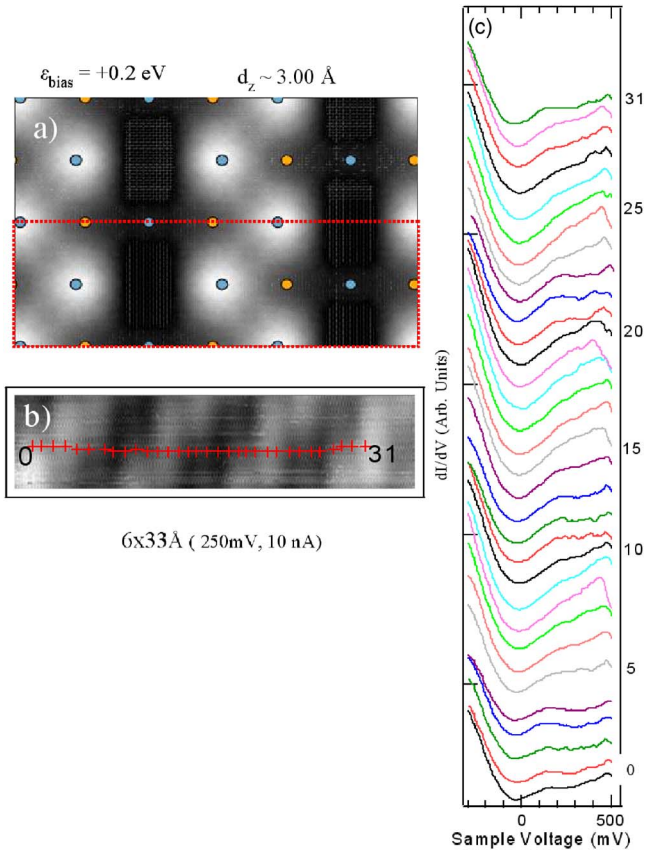

FIG. 8. (Color online) (a) Simulated STM image of the C/Fe(100) $c(3\sqrt{2}\times\sqrt{2})$ surface; blue (yellow) circles indicate Fe (C) atoms, respectively, and white (dark) area correspond to high (low) tunneling current. (b) Topographic STM image (6×33 Å^2) of the zig-zag arrangement (V_b=250 mV, I_t=10 nA). (c) dI/dV-V spectra measured at the points indicated by the markers (+) in the image of (b). The bottom (top) spectra correspond to the left (right) markers in the image, as indicated by the numbers from 1 to 31. The spectra were taken with lock-in amplifier (f_{mod}=4.3 kHz, V_{mod} =10 mV) and the tip-sample distance was set as the same of image acquisition. The spectra on the white zig-zag chain show a shoulder at $V=+150/200$ mV.

toring the oxygen uptake of the surface by means of photoemission intensity at 6 eV binding energy (mostly O 2p states) shows at least an order of magnitude reduced sticking coefficient of the C/Fe(100) surface with respect to the reference pristine Fe(100) surface. A reduced number of dangling bonds on the surface is also suggested in the STM images by the white clouds localized at C-chain breaks, which may represent the residual number of unsaturated bonds available for chemisoprtion of contaminants. The C 1s line shape in the segregated surface loses all high BE structures associated with graphitic or carbidic C, which are present after ion sputtering as residual surface impurities, but presents an asymmetric line shape that can be described by the overlap of at least three components and an asymmetric tail due to the metallic environment (Doniac-Sunjic lineshape). These components are spread over 400 meV and should be attributed to C in quite different configurations at the surface. By means of Auger electron spectroscopy it is further confirmed that the C/Fe abundance ratio at the surface is well defined and characteristic of the associated LEED patterns showing $c(2\times2)$ and $c(3\sqrt{2}\times\sqrt{2})$ ordered domains. Furthermore, Auger spectra suggest a strong C-Fe bond from the presence of the two structured Auger lines at the low kinetic energy side with respect to the main line, in agreement with previous results.[33,34] The change in reconstruction does not imply that other coordination sites of the Fe(100) surface should be considered, but that a change in C coverage, due to the thermal process, leads to a rearrangement of the C atoms on hollow sites, as confirmed by our *ab initio* calculation and as reported in literature.[28,31]

B. Zig-zag chain structure

The STM images give evidence of the formation of stripes in the [110] and [1-10] directions with a zig-zag fine structure, in correspondence with the long-range order of the reconstructed mesoscopic domains. Parallel stripes terminate at some boundaries characterized by higher electron densities, which behave like dislocations since the network of parallel stripes on the opposite side is laterally shifted. Other stripes form cose mazes by rotating sharply between the ortogonal directions either without measurable charge density changes or with evidence of higher charge density at the corners. The images are quite dependent on the bias voltage, i.e., on the nature of the electron states mostly involved in the tunnelling. While the evidence of the stripe arrangements and of their zig-zag chain fine structure is obtained here for the first time, it is not straightforward to associate the imaged charge density with atomic species and absolute positions. Nevertheless a geometrical model of the surface structure compatible with the STM observations can be derived yielding a hypothesis of the unit cell of the structure that can be taken as the starting point for a total energy analysis. Moreover, zig-zag chains do avoid each other, never cross one another, and are laterally shifted after a break point or boundary. This behavior indicates an overall repulsive force between adjacent chains and a gain in making a 90 deg turn instead of crossing another chain. The breaking points are always marked by a high current density in the STM. This indicates that some sort of unsaturated bond remains at the end of a chain which, in turn, indicates that the iron bands are heavily hybridized in the chain structure, such as to produce local defects where it merges into unreconstructed areas, or just boundaries with other domains. The observed buckling of the chains does not seem to justify a large energy difference as measured in the C 1s photoemission. We therefore attribute only one component of the C 1s to the carbon in the striped domains and the remaining components in unreconstructed or boundary areas.

Ab initio calculations corroborate the description of the C zig-zag chain structure. The results show that indeed the C atoms occupy the fourfold hollow sites of Fe(100) with fivefold C-Fe coordination, consistent with recent results.[23,32] Both the $c(2\times2)$ and the $c(3\sqrt{2}\times\sqrt{2})$ reconstructions, at C coverage of $\frac{1}{2}$ and $\frac{2}{3}$ atomic layers, respectively, are compatible with the same C sites, and the repulsive C-C interaction favors one or the other reconstruction as a function of C

density. The C atoms lie almost inside the surface: they are ~0.2–0.3 Å above the uppermost iron layer. The distance of the carbon from the iron atom underneath is 1.89 Å. The Fe atoms laterally confined within the stripes are slightly higher than those that sit between the stripes. The chain structure is favored, with an optimal configuration for double zig-zag chains (Figs. 7 and 8). We note, however, that the inequivalence of the two sites in the zig-zag chain, inferred from the STM measurements, is not present in the equilibrium atomic structure predicted by the *ab initio* calculations. Our calculations are performed for an ideal, infinitely extended $c(3\sqrt{2}\times\sqrt{2})$ reconstructed surface and do not take into account the finite size of the reconstructed domains. The domain boundary effects may not be negligible for domains of nanometer lateral size and may account for unexplained features like the experimentally observed buckling within the stripes. Details of the Fermi surface may be responsible for the apparent corrugation from the STM cross sections and will be the object of further study.

C. Identification of the chemical species in the STM

It is not possible to go beyond this phenomenological description of the $c(3\sqrt{2}\times\sqrt{2})$ structure without a definite identification of the chemical species in the STM images. The zig-zag signal in the STM images could, in principle, represent either the location of the C or of the displaced Fe. *Ab initio* calculations were therefore performed to simulate the STM images, corresponding the atomic structure in Fig. 6, by sampling the local density of states at a given tip-surface distance. In Fig. 8(a), we show the simulated STM image for a bias of +200 mV and a tip-surface distance of ~3 Å. Blue and yellow circles represent, respectively, Fe and C atoms, and white (black) areas correspond to high (low) tunneling current. Comparison between the simulated and the experimental images [Fig. 4(c)] indicates that the maxima, displaying a zig-zag distribution in the STM, are located on the iron atoms enclosed within the C stripes. We note that the calculated images do not qualitatively change up to +800 mV bias and for all tip-surface distances considered, i.e., from 2.6 to 3.2 Å. The tunneling current, for biases in the range 0.3 to 0.7 V, can be mainly ascribed to Fe surface states laterally confined by the C stripe. These states have been investigated *ab initio* in Ref. 35 and correspond to one-dimensional states located on the Fe atoms in the C/Fe stripes, with $d_{3z^2-r^2}$ symmetry. At positive biases lower than 0.3 V, other states from the Fe bands, rehybrizided in the chain structure, are found to contribute significantly to the zig-zag chain signal. The iron $d_{3z^2-r^2}$ surface states have been shown to be responsible for a prominent peak at ~0.2 eV above E_F in STS measurements on the clean Fe(001) surface.[26] The *ab initio* calculations in Ref. 35 indicate that, in the presence of the C chains, such states are shifted to higher energy and give rise to surface state bands of one-dimensional character. Similar confinement and shifts to higher energy were also observed experimentally in related surfaces with segregated impurities.[27,28,36,37]

Using scanning tunneling spectroscopy, we have investigated the local density of states, across the stripes, for biases in the range −300 to +500 mV. Figure 8(b) shows the high resolution STM image of the zig-zag chain (33×6 Å^2) and Fig. 8(c) the STS spectra, where the dI/dV curves numbered from 0 to 31 (bottom to top) were measured at positions marked by the crosses in panel (b). At positive voltage, we observe a shift to higher energy in the spectral weight of the curves corresponding to the black areas in panel (b), compared to those in the white area, which is consistent with the calculated trend.[35] On the other hand, the spectra corresponding to the white areas in panel (b) display a shoulder at $V=+150/200$ mV, which differs from the calculated behavior. Although a shoulder is present in the simulated spectra,[35] it is located at lower bias (zero bias). The comparison between theory and experiment is thus not fully conclusive concerning the spectroscopic features, and further investigations at higher bias and/or using spin-polarized STS would be needed to experimentally confirm the theoretical assignment of the tunneling current.

V. CONCLUSIONS

The segregation of carbon from bcc Fe to the (100) surface leads to the occupancy of the fourfold hollow by C, in fivefold coordination with Fe neighbors. The bonds between C and Fe are strong, but the C-C repulsion plays a key role in establishing the local and long-range structure as a function of the relative aboundancy of C and Fe in the surface. The $c(3\sqrt{2}\times\sqrt{2})$ phase corresponds to the formation of carbon stripes arranged in a way to avoid close packing and crossing, extending along the [110] and [1-10] directions. Most of the C atoms belong to these stripes, but minority species exist since the reconstructed domains are rather small, of the order of a few nanometers. The *ab initio* results for the $c(3\sqrt{2}\times\sqrt{2})$ C zig-zag chain structure indicate that C atoms are strongly bound to the Fe surface at the hollow sites, with an equilibrium position only 0.2 Å above the outermost Fe surface atoms. The repulsive C-C nearest-neighbor interactions, heuristically assumed in Monte Carlo simulations[7] to account for the experimentally $c(2\times2)$ surface reconstruction (C coverage of $\frac{1}{2}$ ML), is confirmed in the present study: the zig-zag chains, corresponding to a coverage of $\frac{2}{3}$ ML, can be understood as a consequence of the repulsive interactions between the C occupying the hollow sites. The $c(3\sqrt{2}\times\sqrt{2})$ phase, albeit chemically metastable, is characterized by distinct electronic properties, with rehybridization of the iron *s-d* states and the formation of Fe surface state bands of one-dimensional character due to the lateral confinement by the C stripes. The reactivity of the C/Fe(100) surface to impinging molecules, namely O_2 and CO, is greatly reduced with respect to the pristine Fe(100) surface, and the segregation of P leads to selective surface sites corresponding to the "defects" in the C/Fe(100) stripe. Certainly this electronic structure is caracteristically different from that of clean Fe(100) and one should investigate its magnetic properties, since a one-dimensional confinement may influence the band narrowing, which makes the Fe(100) clean surface a strong ferromagnet, differently from bulk bcc iron.

ACKNOWLEDGMENTS

We are grateful to Massimo Altarelli for continuous support. G.P. thanks F. Sirotti and P. Torelli (LURE) and M. Cantoni (Politecnico di Milano) for valuable suggestions as well as for the use of their samples. Authors wish to express their thanks to D. Krizmancic for the software support. The *ab initio* calculations presented in this work are based on the pwscf code.[38] GT and NB acknowledge support by the INFM within the framework of the "Iniziativa Trasversale di Calcolo Parallelo."

---

*Present address: CNR-Istituto dei Sistemi Complessi, via Salaria, Km.29.3, 00016 Montelibretti (RM), Italy.

[1] For a review article, see, e.g., F. J. Himpsel, K. N. Altmann, R. Bennewitz, J. N. Crain, A. Kirakosian, J. L. Lin, and J. L. McChesney, J. Phys.: Condens. Matter **13**, 11097 (2001).
[2] L. Proville, Phys. Rev. B **64**, 165406 (2001).
[3] L. Proville, Phys. Rev. Lett. **88**, 046102 (2002).
[4] M. Sotto and B. Croset, Surf. Sci. **461**, 78 (2000).
[5] H. J. Grabke and H. Viefhaus, in *Surface Segregation and Related Phenomena*, edited by P. A. Dowben and A. Miller (CRC Press, Boca Raton, FL, 1990).
[6] For a textbook, see A. Zangwill, *Physics at Surfaces* (Cambridge University Press, Cambridge, UK, 1988).
[7] C. Uebing, Phys. Rev. B **50**, 12138 (1994).
[8] H. J. Grabke, W. Paulitschke, G. Tauber, and H. Viefhaus, Surf. Sci. **63**, 377 (1977).
[9] A. Biedermann, M. Schmid, and P. Varga, Phys. Rev. B **50**, 17518 (1994).
[10] S. K. Kim, C. Petersen, F. Jona, and P. M. Marcus, Phys. Rev. B **54**, 2184 (1996).
[11] K. O. Legg, F. Jona, D. W. Depsen, and P. M. Marcus, Surf. Sci. **66**, 25 (1977).
[12] J. Fujii, M. Galaktionov, L. Giovanelli, G. Panaccione, F. Bondino, I. Vobornik, and G. Rossi, Thin Solid Films **428**, 30 (2003).
[13] For further information, see http://ape.tasc.infm.it.
[14] J. P. Perdew, K. Burke, and M. Ernzerhof, Phys. Rev. Lett. **77**, 3865 (1996).
[15] D. Vanderbilt, Phys. Rev. B **41**, R7892 (1990).
[16] A. Dal Corso and S. de Gironcoli, Phys. Rev. B **62**, 273 (2000).
[17] F. Favot and A. Dal Corso, Phys. Rev. B **60**, 11427 (1999).
[18] The Fe and C pseudopotentials were generated using the parameters reported in Refs. 16 and 17, respectively.
[19] H. J. Monkhorst and J. D. Pack, Phys. Rev. B **13**, 5188 (1976).
[20] G. Trimarchi and N. Binggeli, unpublished.
[21] J. F. Morar, F. J. Himpsel, G. Hollinger, J. L. Jordan, G. Hughes, and F. R. McFeely, Phys. Rev. B **33**, 1340 (1986).
[22] This behavior is a function of two parameters: temperature and time of annealing. Figure 1 reports the evolution of the line shapes obtained by setting the maximum value of temperature for a fixed amount of time.
[23] V. Blum, A. Schmidt, W. Meier, L. Hammer, and K. Heinz, J. Phys.: Condens. Matter **15**, 3517 (2003).
[24] P. Sautet, J. C. Dunphy, and M. Salmeron, Surf. Sci. **364**, 335 (1996); J. C. Dunphy, P. Sautet, D. F. Oegletree, and M. B. Salmeron, J. Vac. Sci. Technol. A **11**(4), 1975 (1993).
[25] D. Jentz, S. Rizzi, A. Barbieri, D. Kelly, M. A. van Hove, and G. A. Somorjai, Surf. Sci. **329**, 14 (1995).
[26] J. A. Stroscio, D. T. Pierce, A. Davies, R. J. Celotta, and M. Weinert, Phys. Rev. Lett. **75**, 2960 (1995).
[27] A. Biedermann, O. Genser, W. Hebenstreit, M. Schmid, J. Redinger, R. Podloucky, and P. Varga, Phys. Rev. Lett. **76**, 4179 (1996).
[28] M. M. J. Bischoff, C. Konvicka, A. J. Quinn, M. Schmid, J. Redinger, R. Podloucky, P. Varga, and H. van Kempen, Phys. Rev. Lett. **86**, 2396 (2001).
[29] J. J. Yeh and I. Lindau, At. Data Nucl. Data Tables **32**, 1 (1985).
[30] J. Fujii and G. Panaccione, unpublished results.
[31] A. Biedermann, M. Schmid, and P. Varga, Surf. Sci. **331**, 787 (1995).
[32] D. E. Jiang and E. A. Carter, Phys. Rev. B **71**, 045402 (2005).
[33] F. Sette, G. K. Wertheim, Y. Ma, G. Meigs, S. Modesti, and C. T. Chen, Phys. Rev. B **41**, 9766 (1990); Surf. Sci. Spectra **1**, 297 (1993).
[34] R. Rosei, F. Ciccacci, R. Memeo, C. Mariani, L. S. Caputi, and P. Papagno, J. Catal. **83**, 19 (1983).
[35] G. Trimarchi and N. Binggeli, cond-mat/0508129; Phys. Rev. B **72**, 081408(R) (2005).
[36] T. Kawagoe, E. Tamura, Y. Suzuki, and K. Koike, Phys. Rev. B **65**, 024406 (2005).
[37] S. Heinze, X. Nie, S. Blügel, and M. Weinert, Chem. Phys. Lett. **315**, 167 (1999); S. Ohnishi, A. J. Freeman, and M. Weinert, Phys. Rev. B **28**, 6741 (1983).
[38] S. Baroni, A. Dal Corso, S. de Gironcoli, and P. Giannozzi, http://www.pwscf.org.